Interdecadal Change in the Relationship between ENSO and the Intraseasonal Oscillation in East Asia

KYUNG-SOOK YUN, KYONG-HWAN SEO, AND KYUNG-JA HA

Division of Earth Environmental System, Department of Atmospheric Sciences, College of Natural Science, Pusan National University, Busan, South Korea

(Manuscript received 15 September 2009, in final form 19 February 2010)

ABSTRACT

The northward-propagating intraseasonal oscillation (NPISO) during the boreal summer is closely linked to the onset/retreat and intensity of the East Asian summer monsoon (EASM). In this study, interdecadal variability in the relationships between the NPISO and El Niño–Southern Oscillation (ENSO) was investigated using long-term outgoing longwave radiation data obtained from the 40-yr ECMWF Re-Analysis (ERA-40) for a 44-yr period (1958 to 2001). It was found that before the late 1970s, the preceding winter ENSO influenced the early summer (i.e., May to June) NPISO activity, whereas after the late 1970s a strong relationship appeared during the later summertime (i.e., July to August). The May–June NPISO before the late 1970s was modulated by springtime Indian Ocean sea surface temperature warming and central North Pacific suppressed convection anomalies and was consequently related to the ENSO-induced west Pacific (WP) pattern, which shows a north–south dipole structure over the North Pacific from winter through spring. After the late 1970s, because of an anomalously strengthened Walker–Hadley circulation, Indian Ocean SST warming was significantly maintained until summer, which promoted a strong suppressed convection anomaly over the Philippine Sea during summer and consequently an enhanced western North Pacific subtropical high and Pacific–Japan (PJ) pattern.

1. Introduction

A number of studies have reported on the decadal change in the East Asian summer monsoon (EASM) rainfall and its association with the El Niño–Southern Oscillation (ENSO) (Gong and Ho 2002; Wu and Wang 2002; Wang et al. 2007; Ha and Lee 2007). In addition, Goswami and Mohan (2001) showed that the interannual and decadal variabilities were closely related to the variability in the intraseasonal oscillation (ISO), an essential part of the Asian monsoon system. It has also been recognized that the ISO not only modulates the timing of the onset and retreat of the monsoon system (e.g., Lau and Chan 1986) but also influences the interannual variability of a monsoon through changes in the annual structure (Ha and Ha 2006).

Unlike the boreal winter ISO, which is propagated to the east, the boreal summer ISO is characterized by northward or northwestward propagation over the Indian Ocean and western North Pacific (WNP), as well as eastward propagation along the equator (e.g., Kemball-Cook and Wang 2001; Seo et al. 2007, 2009). Several mechanisms for the northward-propagating ISO (NPISO) have been proposed with causal processes such as the surface hydrology (e.g., Webster 1983), air–sea interactions (e.g., Kemball-Cook and Wang 2001), Rossby wave emanation from enhanced deep convection (e.g., Wang and Xie 1997; Hsu and Weng 2001), and an easterly vertical wind shear (Jiang et al. 2004). Regarding the northward-propagating characteristics, the boreal summer ISO is not trapped in the tropics and exhibits a significant signal in the extratropics, especially over the WNP region (Kawamura et al. 1996; Kang et al. 1999). Yun et al. (2008) recently showed that the boreal summer NPISO over the EASM region was significantly affected by the preceding winter ENSO, unlike the insignificant relationship between the winter ISO activity and ENSO (Hendon et al. 1999; Slingo et al. 1999). They reported a possible link to the springtime Indian Ocean sea surface temperature (SST) warming via Walker circulation. This warming induces a suppressed convection

Corresponding author address: Kyung-Ja Ha, Department of Atmospheric Sciences, Pusan National University, Busan, South Korea.
E-mail: kjha@pusan.ac.kr

DOI: 10.1175/2010JCLI3431.1

over the Philippine Sea, which then induces an anomalous western North Pacific subtropical high (WNPSH), leading to a Rossby wave train and enhanced NPISO activity over Korea and Japan. On the other hand, Teng and Wang (2003) and Kim et al. (2008) suggested that the tropical NPISO activity over the WNP showed somewhat different characteristics from the NPISO in the EASM, since the former is associated with the developing ENSO phase during the summer.

The link between EASM rainfall and ENSO (Chang et al. 2000; Terao and Kubota 2005; Li et al. 2007) suggests that the NPISO and ENSO relationship should be documented more clearly. Since the late 1970s, ENSO has experienced a significant climate shift (Trenberth and Hurrell 1994; Wang 1995; Zhang et al. 1997). Although some evidence for a decadal or interdecadal change for the ISOs (Slingo et al. 1999; Zveryaev 2002) exists, an interdecadal change after the late 1970s in the ISO–ENSO relationship has received little attention. The present study reports on an investigation into the interdecadal change in the relationship between ENSO and NPISO in the EASM system. To examine the long-term variability in the NPISO, outgoing longwave radiation (OLR) data, obtained from the 40-yr European Centre for Medium-Range Weather Forecasts (ECMWF) Re-Analysis (ERA-40) data from 1958 to 2001, were used. The possible mechanism associated with the change in the relationships between the circulation over the WNP region and the NPISO is discussed.

2. Data and methodology

To identify the NPISO for a long-term period, OLR data obtained from the ERA-40 dataset from 1958 to 2001 were used (Uppala et al. 2005). Because of the inclusion of satellite observations in an assimilation scheme since 1979, the ERA-40 reanalysis data may include some systematic biases in the OLR data prior to this date (e.g., Quan et al. 2003). However, from a comparison with the previous results derived from in situ observations (e.g., Hu 1997; Chang et al. 2000), it is believed that those from the ERA-40 data reasonably represent the interdecadal change in the EASM after the late 1970s. In addition, the interdecadal change in the NPISO–ENSO relationship obtained from the ERA-40 data shows good agreement with the National Centers for Environmental Prediction–National Centers for Atmospheric Research (NCEP–NCAR) reanalysis data (hereafter called NCEP data) between 1948 and 2008 (Kalnay et al. 1996). To evaluate the OLR data from ERA-40, the power spectrum analyses from both OLR data obtained from National Oceanic and Atmospheric Administration (NOAA) satellite observations and the ERA-40 dataset between 1979 and 2001 year were initially compared (not shown). The 7-day moving average OLR anomalies from both datasets showed equivalently significant 30–60-day periodicities over the EASM region (Lau et al. 1988).

Prior to investigating the change in NPISO–ENSO relationship, the change in the intraseasonal variance (ISV) was examined in the WNP–EASM system. The NPISO, particularly the 30–60-day oscillation, is an important component of the ISV of summer convection (Lau and Chan 1986). Since the NPISO activity affects the ISV, the interannual and interdecadal variabilities in the ISV could be significantly related to interdecadal change in NPISO activity over the East Asia. The ISV can be represented as the variability in the daily OLR anomaly during a season [May–October (MJJASO)]. First, the interannual variability of the ISV can be seen as an empirical orthogonal function (EOF) for the spatial distribution of the ISV, as shown in Fig. 1. From the first principal component (PC) time series, it can be seen that the ISV has magnified over the WNP region after the late 1970s (Fig. 1a). The second EOF mode shows some decadal variation but explains only 12% of the total variance, half that of the first mode (Fig. 1b). The strengthening of the ISV over the WNP–EASM region may affect the interdecadal change of the ISO. A better understanding of the remote impact of the variation of SST over the tropics on ISO variability is, of course, very important in improving the predictability of a monsoon's intensity.

The ISO is manifested as a seesaw pattern along ~22°N between the WNP summer monsoon and EASM regions (e.g., Mao et al. 2010). Yun et al. (2009) have shown that the ISO phase in the EASM system is opposite to that in the WNP summer monsoon. To highlight the ISO over East Asia, an EOF analysis of the 30–60-day bandpass-filtered OLR data was applied in the spatial domain over the EASM (22.5°–45°N, 100°–150°E) and in the temporal range from May to October, which is identical to that conducted in the study of Yun et al. (2008).

The ERA-40 and Hadley Centre Sea Ice and Sea Surface Temperature (HadISST) datasets (Rayner et al. 2003) between 1958 and 2001 were used to detect the interdecadal change in NPISO–ENSO relationships. For selecting ENSO years, the monthly Niño-3 (5°S–5°N, 90°–150°W) SST index was derived from Climate Prediction Center (CPC)–NOAA data. To achieve the same sample size for comparison, the change between two epochs, 1958–79 (the first period) and 1980–2001 (the second period), were investigated. Note that 1979 was considered a transition year in the previous studies of Gong and Ho (2002) and Wang et al. (2008).

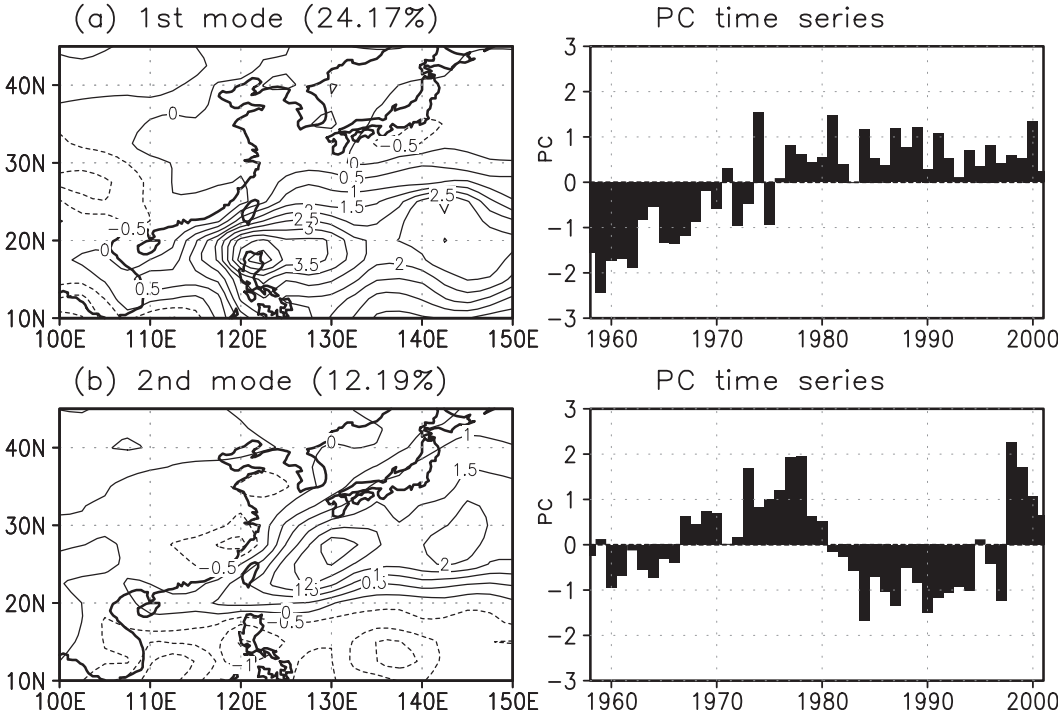

FIG. 1. The spatial patterns and their associated PC time series for the (a) first and (b) second EOF modes obtained from the intraseasonal variance in the OLR data during the extended summer (MJJASO) for 1958–2001.

3. The NPISO activity and its ENSO relationship

The NPISO has been identified as the first two leading EOF modes, and its activity is computed by the variance of the PC time series in the first two EOF modes from the 30–60-day filtered OLR. The seasonal variance of the NPISO activity was estimated using a 91-day moving average of the NPISO activity. The first two EOF results given by the ERA-40 data between 1958 and 2001 are shown in Figs. 2a and 2b, respectively. The first two leading PCs are significantly correlated with each other at a lag of ~10 days and well separated from higher modes (according to North et al. 1982). Consequently, the NPISO is characterized by a dominant period of ~40 days. Figure 2c shows the interannual variability of the seasonal NPISO activity (i.e., 91-day running mean NPISO variance) for the two months of July and August. Note that some extreme years (e.g., 1998) account for a significant portion of the interannual variability of the NPISO activity.

To detect the interdecadal change in the NPISO–ENSO relationship, the sliding correlation coefficient between the July–August NPISO activity and its contributing factor (i.e., the Niño-3 index and WNP subtropical high) was calculated. Here, the WNPSH denotes June–August (JJA) 850-hPa geopotential height anomalies averaged over the domain 15°–25°N, 120°–170°E. The correlation coefficients between the NPISO activity and the two mentioned factors were calculated for the period between 1958 and 2001, with a 15-yr window (Fig. 2d). After about the late 1970s, the relationship between the NPISO activity with the Niño-3 SST index and the WNPSH increased dramatically. A statistically significant positive correlation of ~0.6 has become particularly evident in recent years. Although the NPISO activity exhibits no prominent variation on the interdecadal time scale (see Fig. 2c), the rapid change that appeared in the sliding correlation reflects the differing NPISO–ENSO relationships before and after the late 1970s. To validate the results from the ERA-40 data, the sliding correlation coefficients between the ENSO and NPISO activity based on the NCEP reanalysis data and NOAA data are shown in Fig. 3, which shows an almost identical interdecadal change to those from the ERA-40 reanalysis data.

The decadal change in the relationships between the two sequences of 1958–79 and 1980–2001 can be seen in the correlation coefficients between the monthly NPISO activity during the extended summer season (MJJASO) and the Niño-3 SST index with time lags spanning from −24 to +24 months (Fig. 4). Note that a negative lag indicates that ENSO precedes the NPISO activity. In the second period (i.e., 1980–2001), a strong positive correlation is found during the months of June to September with the preceding winter Niño-3 index. Although the

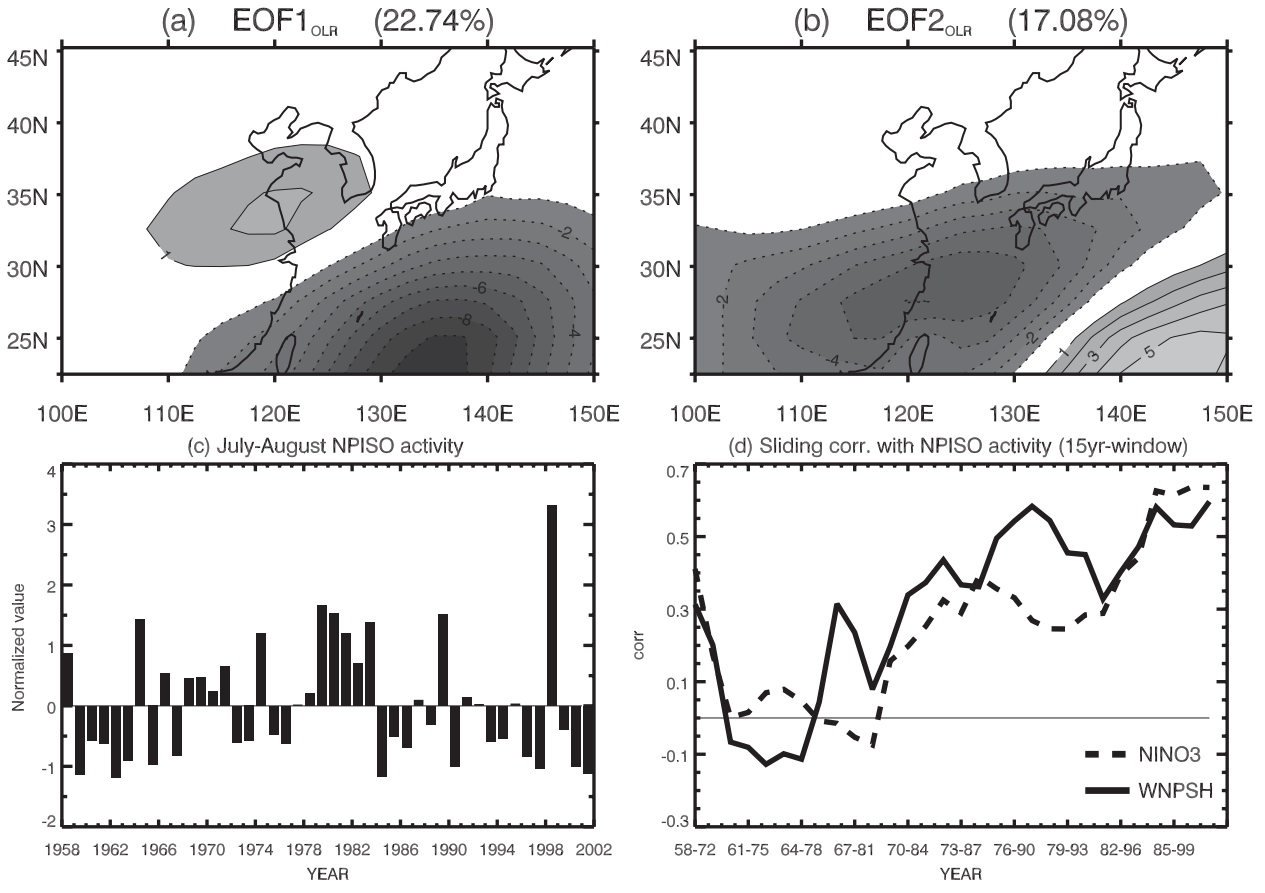

FIG. 2. (a),(b) The spatial patterns for the (a) first and (b) second EOF modes obtained from the 30–60-day filtered OLR data during the extended summer (MJJASO) for 1958–2001 [adapted from Yun et al. (2008)]. (c) Interannual variability of the July–August averaged NPISO activity from 1958 to 2001. (d) Sliding correlation coefficient between the July–August NPISO activity and the NDJ Niño-3 index (dashed line) and the JJA WNPSH anomalies (solid line), using a 15-yr window.

peak correlation is shifted slightly into July, the relationship is reasonably consistent with the results reported by Yun et al. (2008), indicating that the preceding winter ENSO leads to the summer NPISO in the EASM. Conversely, the first period (i.e., 1958–79) shows a relatively weak positive correlation in the months of May to June. This suggests that in the second period, the dynamical relationship between the NPISO and ENSO

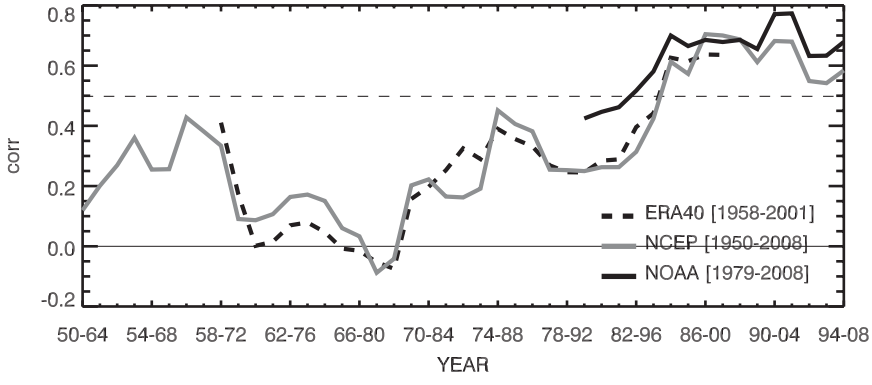

FIG. 3. Sliding correlation coefficient between the July–August NPISO activities obtained from the ERA-40 (dashed line), NCEP (gray line), and NOAA (solid line) OLR and the NDJ Niño-3 index, with a 15-yr window.

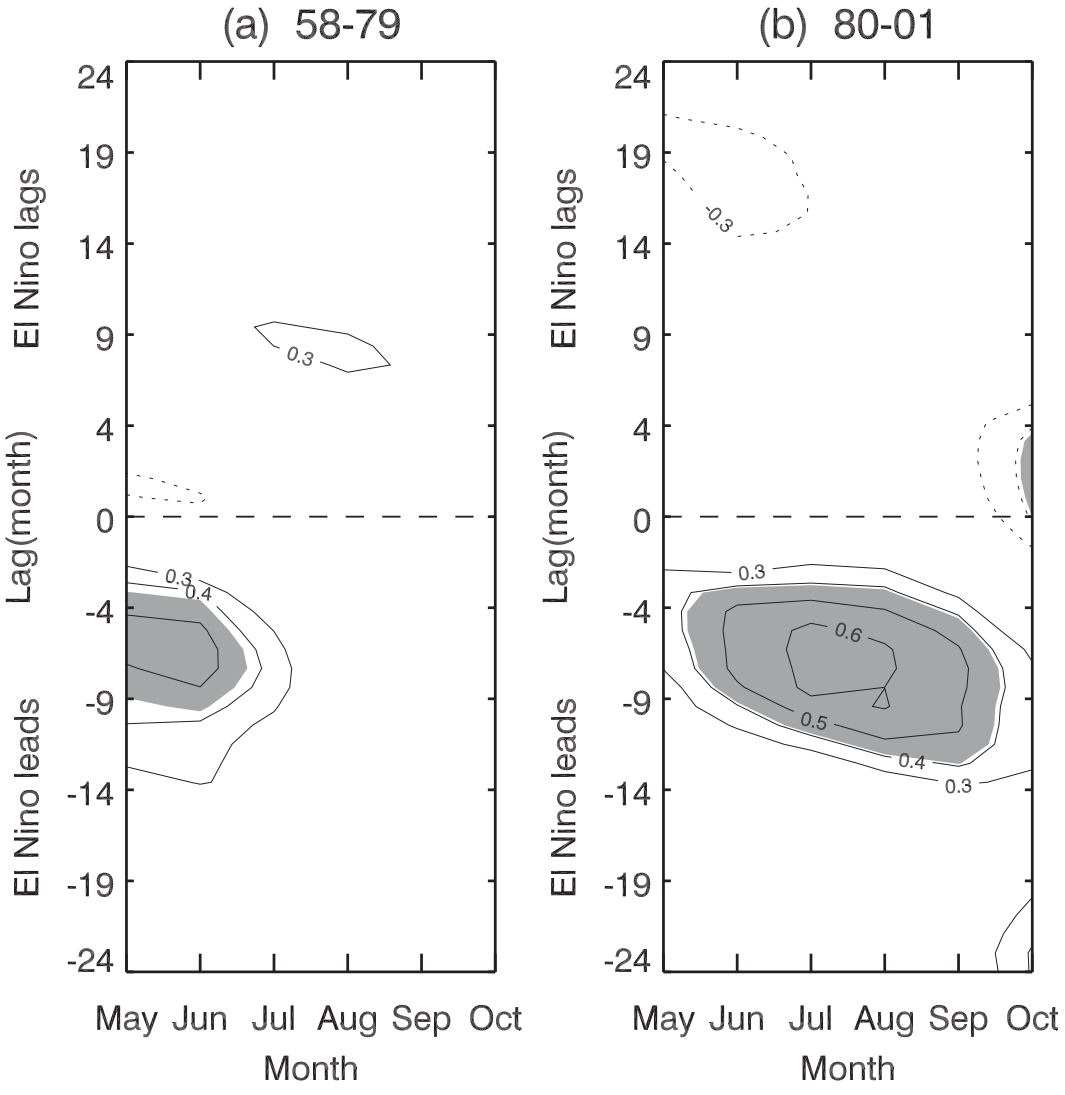

FIG. 4. Lag–lead correlation coefficients between the monthly NPISO activities for MJJASO and the monthly Niño-3 SST index during the years (a) 1958–79 and (b) 1980–2001. Only coefficients significant at the 95% confidence level are shaded.

becomes stronger, with its maximum appearing later than that in the first period. In the following section, the interdecadal change will be investigated in terms of the May–June and July–August NPISO activities.

4. The connections among IOSST, WNPSH, and NPISO activity

Yun et al. (2008) emphasized the importance of the WNPSH in the NPISO–ENSO relationship. In this section attempts were made to determine how ENSO influences the NPISO. For this, the regressed map for the 850-hPa geopotential height and vertically integrated moisture transport anomalies for the April–June (AMJ) against the May–June NPISO activities and for the June–August against the July–August NPISO activities in the first and second periods, respectively, was calculated (Fig. 5). During the second period, the WNPSH anomaly is formed over the domain 10°–30°N, 110°–180°E (Fig. 5b). Along the western edge of the anticyclone, moisture is transported northeastward into East Asia and converges into the cyclonic center located over northeastern Asia. To the north of the low pressure anomaly, a high pressure anomaly, whose center is more than 8 m, emerges over the Okhotsk Sea. During the period 1958–79, however, no significant anticyclonic anomalies exist over the WNP region (not shown). In the first period, the early summer NPISO is modulated not by the summer height structure but rather by that of the late spring (April–June) (Fig. 5a). In comparison

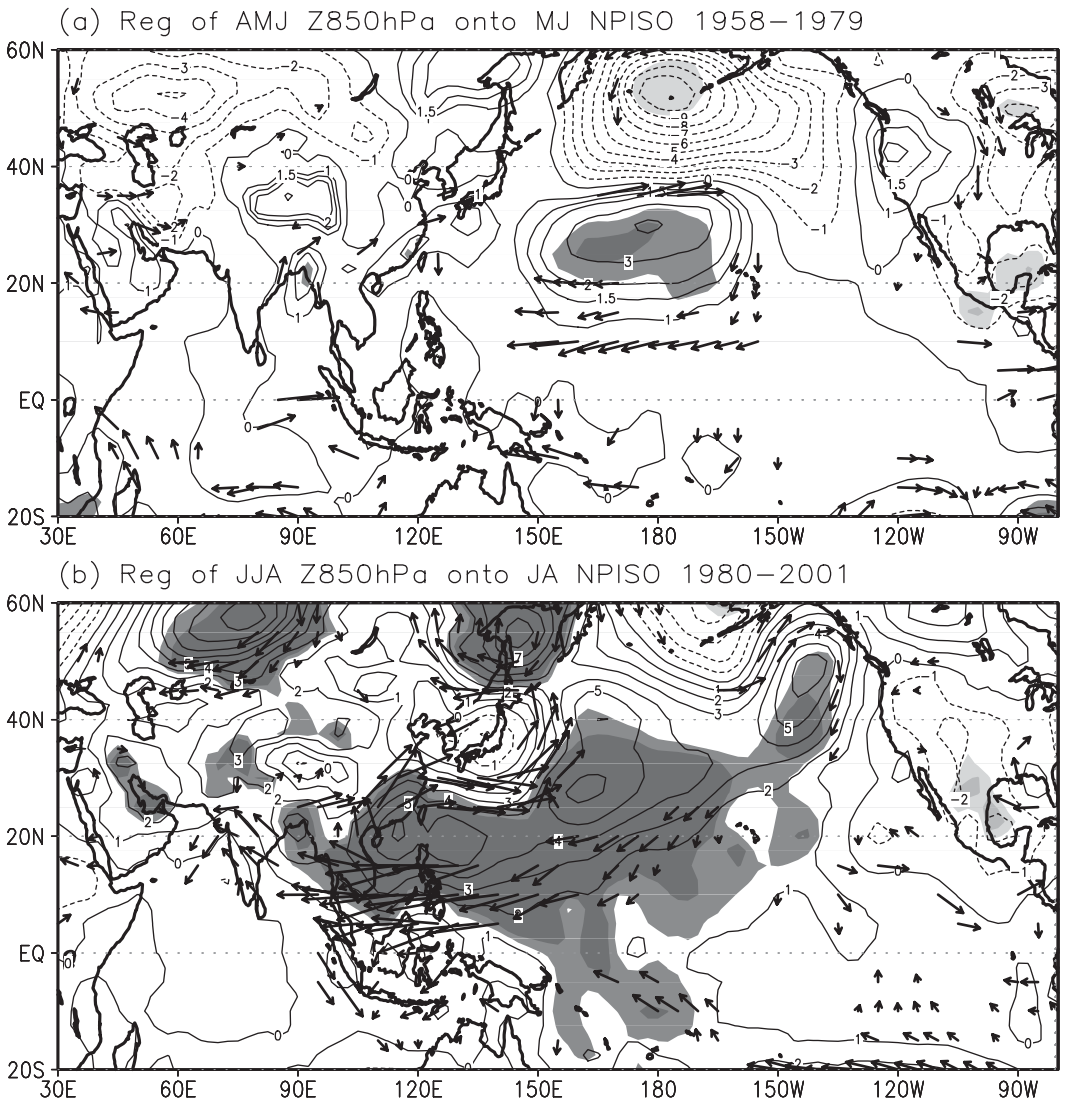

FIG. 5. The regressed field for (a) the April–June 850-hPa geopotential height anomalies against the May–June NPISO activity during years 1958–79 and (b) the JJA 850-hPa geopotential height anomalies against the July–August NPISO activities during the years 1980–2001. The arrows represent the vertically integrated anomalous moisture transport (kg m^{-1} s^{-1}) significant at the 90% confidence level. Heavy (light) shading denotes positive (negative) height anomalies significant at the 90% and 95% confidence levels.

with the summer height structure regressed onto the July–August NPISO (Fig. 5b), the May–June NPISO is related to the height anomaly shifted to the east. The anomaly pattern shows a north–south dipole structure over the North Pacific, with a positive anomaly located at a location south of ~35°N and a negative anomaly north of ~35°N. Although the height anomaly centers are situated somewhat east, their structure closely resembles the west Pacific (WP) pattern, which has been shown to be significantly influenced by ENSO from winter until spring (Wallace and Gutzler 1981; Horel and Wallace 1981). This suggests that, in the first period, the NPISO–ENSO relationship is modulated by the ENSO-related WP pattern, a different mechanism from that in the second period.

The question arises as to whether the lagged link between the WNP circulation and the winter ENSO maximum could be due to Indian Ocean SST (IOSST) warming via Walker circulation (Yun et al. 2008). To test the decadal change in the link, the sliding correlation coefficient between the contributing factors was calculated, with a 15-yr window (not shown). The relationships among the OLR_ps [i.e., June–August OLR anomalies averaged over the Philippine Sea (5°–20°N,

TABLE 1. The ENSO extreme years keyed to the Niño-3 index.

	First period (1958–79)	Second period (1980–2001)
El Niño	1958, 1966, 1969, 1970, 1973, and 1977	1983, 1987, 1988, 1992, 1995, and 1998
La Niña	1963, 1965, 1968, 1971, 1974, 1975, and 1976	1985, 1986, 1989, 1996, 1997, 1999, and 2000

120°–150°E)] and the Niño-3 index, IOSST anomaly, and WNPSH anomalies appeared to abruptly change such that a significant correlation exists after the late 1970s, but not before. These changes are consistent with those found in previous studies on the interdecadal change of the OLR_ps and WNPSH (e.g., Hu 1997; Gong and Ho 2002; Wu and Wang 2002). This implies that the role of the convection activity over the Philippine Sea and the WNPSH in the second period is considerably larger than that during the first period.

Since the NPISO activity itself does not show any interdecadal change after the late 1970s (see Fig. 2c), the change in the relationship can be attributed to the change in ENSO-related signals. To investigate the difference in the ENSO-induced signals between the two periods, a composite analysis for SST anomalies was performed and keyed on the Niño-3 index. Here, an El Niño (La Niña) year is defined in terms of a Niño-3 index greater (smaller) than 0.5 (−0.5). The selected ENSO years are presented in Table 1. During the preceding winter [November–January (NDJ), the mature phase of ENSO], for both the first and second periods warm anomalies were evident in the eastern-central Pacific and Indian Ocean (Figs. 6a,b). Meanwhile, significant cold anomalies in the western Pacific appeared in both hemispheres only during the second period. The noticeable distinction may be the result of an enhanced positive feedback between the SST anomalies and an atmospheric bridge process (i.e., Walker and Hadley circulations) caused by a warmer mean SST during the latter period (Chang et al. 2000; Wang et al. 2008). The eastern Pacific warm anomalies decayed moderately in the following spring and summer (Figs. 6c–f), whereas only in the second period did the Indian Ocean basinwide warming become stronger. A significant difference for El Niño/La Niña between the two interdecadal periods was particularly evident during the summer months (Figs. 6e,f).

One reason for this significant difference between the two periods arises from the IOSST warming, which tends to persist until the summer (i.e., warming starts later and also ends later) for the first period, but not for the second period. Many previous studies (e.g., Watanabe and Jin 2002; Ding et al. 2010) have reported that persistent IOSST warming plays an important role in modulating the WNPSH and EASM circulation. In addition, the cooling over the WNP from winter to the next spring was more prominent during the second than the first period. The continued IOSST warming may be related to the strong cooling over the WNP via the atmospheric bridges (e.g., Klein et al. 1999). The WNP cooling during the second period may be due to the stronger WNP anticyclonic anomalies. This anticyclonic anomaly cools the ocean to its east (because of enhanced evaporation cooling and turbulence mixing) and warms it to the west (over the South China Sea). On the other hand, the cooling to the east of the anticyclone suppresses convection and latent heating, which further excites descending Rossby waves that enhance the Philippine anticyclone on their westward journey. This WNPSH and WNP cooling provide a positive feedback that sustains both the anticyclonic anomalies (suppressed convection as shown in Fig. 7) and the cooling over the WNP. This air–sea interaction mechanism has been discussed in detail by Wang et al. (2000, 2003).

The enhanced indirect ENSO response after the late 1970s is also shown in the OLR anomaly field (Fig. 7). During January–February in the second period (Fig. 7b), stronger suppressed (enhanced) convection anomalies appear to a large extent over the western (eastern/central) Pacific compared to those in the first period (Fig. 7a). During the ensuing spring, enhanced convection activity in the first period appeared in the central Pacific (Fig. 7c), whereas enhanced convection anomalies are still prominent in the eastern/central Pacific during the second period (Fig. 7d). The suppressed convection anomalies over the WNP in the second period survived until the following summer (Fig. 7f) compared with the convection activity in the first period (Fig. 7e). Consequently, the suppressed convection over the Philippine Sea and enhanced convection over northeastern Asia become conspicuous during the boreal summer (Fig. 7f). This may be due to the persistent IOSST warming and positive feedback between the WNPSH and WNP cooling. Of particular interest is that the suppressed convection pattern was very similar to the spring suppressed convection anomaly in the first period, except for a slight extension to the east. It should be noted that the May–June NPISO activity in the first period is related more to the spring height anomaly than the summer anomaly.

The NPISO–ENSO relationship after the late 1970s can be understood by dynamic processes, characterized by ENSO-induced IOSST warming, summer suppressed convection, and enhanced WNPSH anomalies due to enhanced anomalous Walker–Hadley circulation (Yun et al. 2008). Recently, Xie et al. (2009) demonstrated that the IOSST warming after El Niño decays in spring induces the emanation of a baroclinic Kelvin wave and

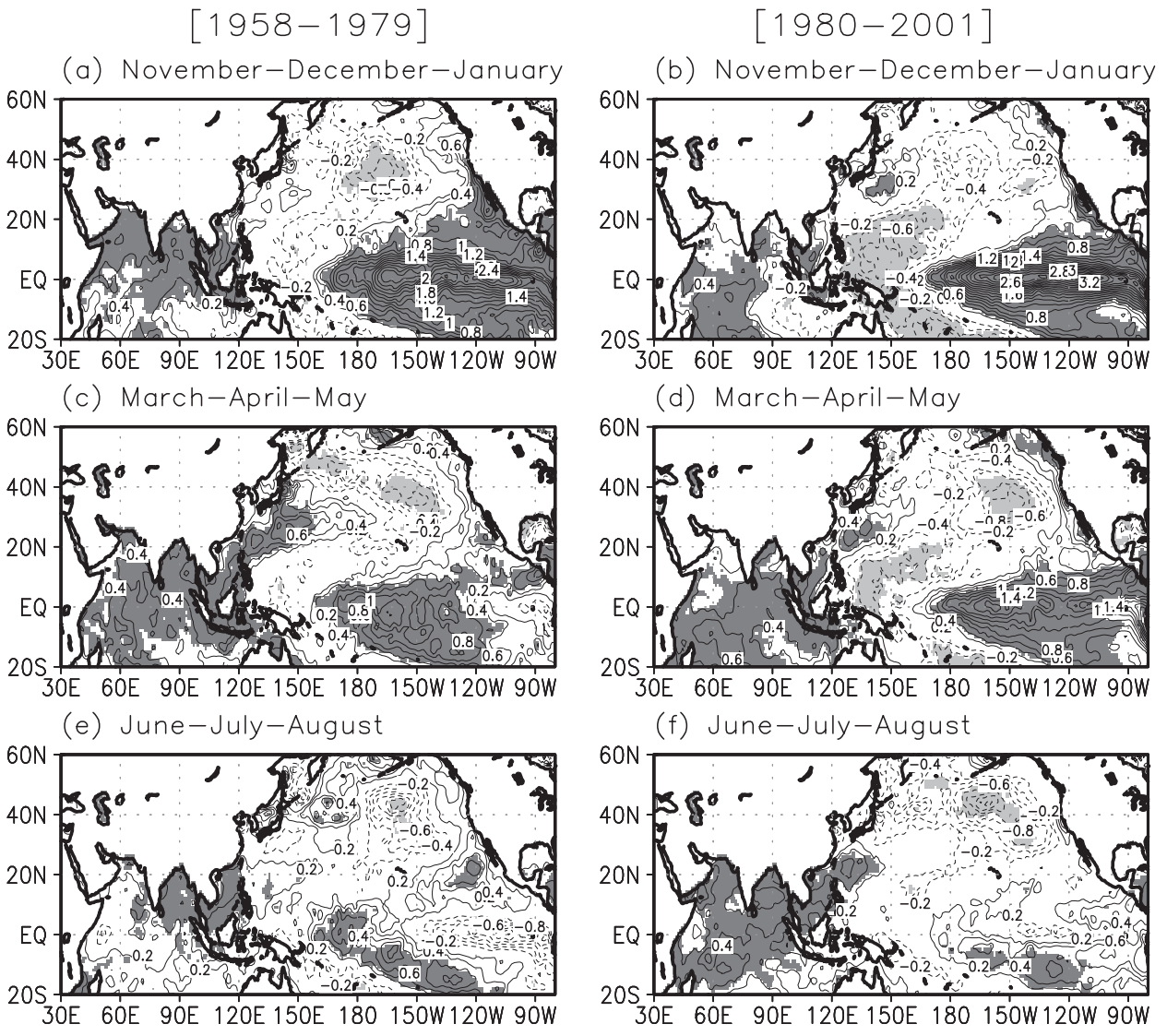

FIG. 6. The composite difference in the SST anomalies from NDJ to JJA for the NDJ El Niño and La Niña during the years (left) 1958–79 and (right) 1980–2001. Shading denotes anomalies significant at the 95% confidence level.

northeasterly wind anomalies into the Pacific, which in turn leads to suppressed convection and the anomalous WNPSH. Before the late 1970s, however, the ENSO-related signals in the SST and OLR anomalies were only evident from the winter to the ensuing spring. If so, how can the early summer NPISO be related to the ENSO phenomena before the late 1970s? To address this question, the spring and summer OLR anomalies against springtime IOSST anomalies averaged over 20°S–20°N, 50°–100°E during the two periods were regressed (Figs. 8a and 8b). As suggested by the data in Figs. 7c and 7f, the spring OLR anomaly in the first period shows a suppressed convection structure over the WNP and is slightly extended toward the east, and the summer convection anomaly is not related to IOSST warming. In the second period, however, the summer regressed field exhibits suppressed convection over the Philippine Sea and enhanced convection to the northeast Asia (Fig. 8b). This can be attributed to a weakened Walker circulation due to the downward motion in the western Pacific. The summertime low-level height field regressed onto this summer OLR_ps displays a well-organized three-cell circulation structure similar to a Rossby wave response to reduced heating, and shows a Pacific–Japan (PJ) pattern (Nitta 1987) (Fig. 8d). The JJA height field regressed onto the IOSST anomaly also exhibits a similar PJ-like structure (Fig. 8f), with a remarkable similarity to these structures gained from the regression to the July–August NPISO activity. On the other hand, in the first period, the spring convection anomaly over 10°–25°N,

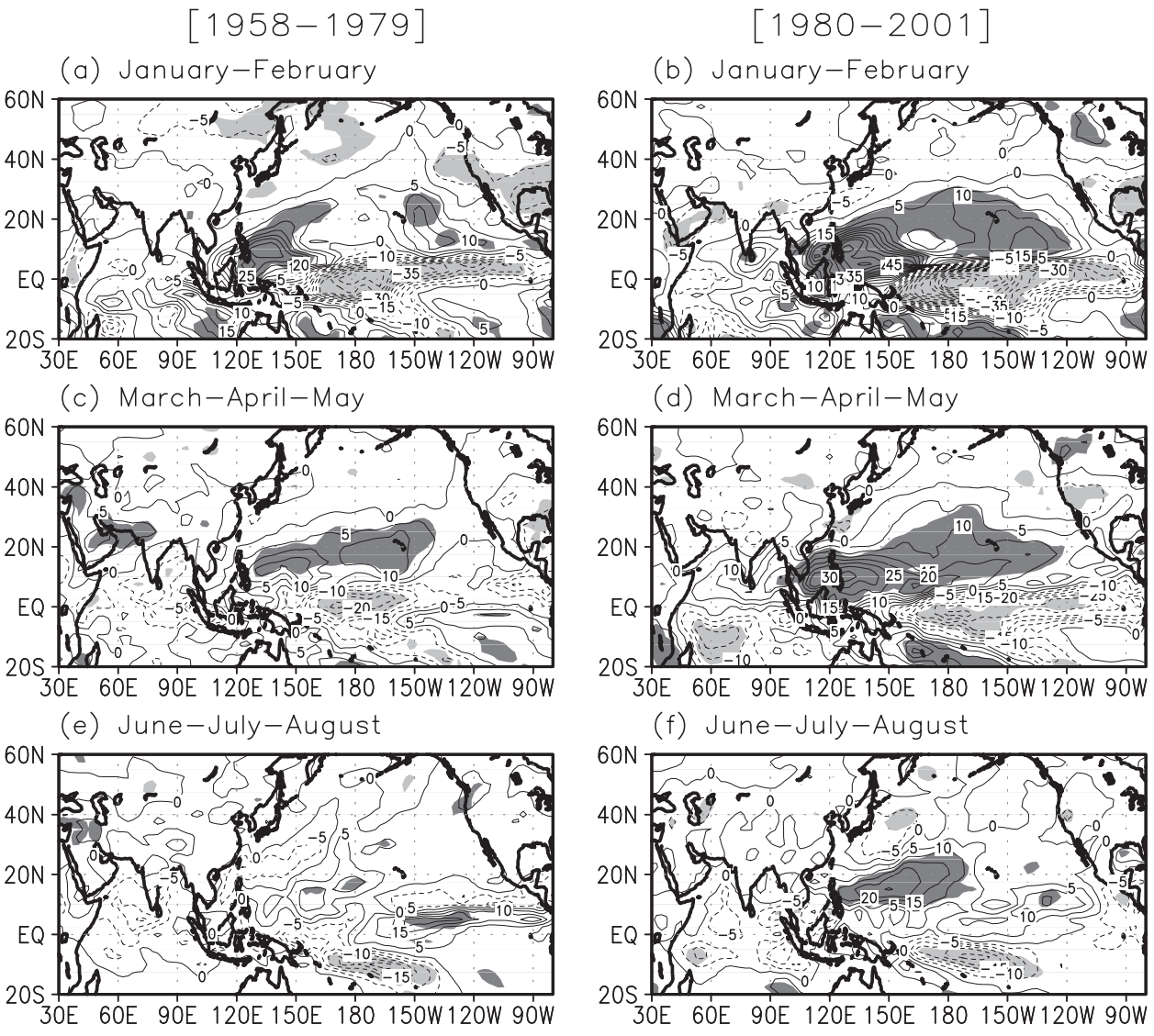

FIG. 7. As in Fig. 6, but for the OLR anomalies.

160°E–150°W, located to the northeast of the WNP anomaly, is stronger. For convenience, the convection anomaly to the central North Pacific OLR (i.e., OLR_cnp) has been referred to. The spring OLR_cnp anomaly generates the north–south dipole pattern of the late spring 850-hPa height anomaly and shows a WP-like pattern (Fig. 8c). The IOSST warming also introduces a similar WP-like height pattern (Fig. 8e). Although a difference in the exact locations of the height anomaly centers exists, an overall dipole structure is prominent in the regressed field, which is indicative of a close relationship between the May–June NPISO activity and the ENSO-related WP pattern.

In summary, in the second period, the July–August NPISO is closely connected to a PJ pattern, whereas in the first period the May–June NPISO is associated with a WP pattern. To examine this, the sliding correlation, with a 15-yr window, is displayed in Fig. 9 for the NPISO activity and the two teleconnection indices. Here, the WP index was obtained from the CPC Web site (http://www.cpc.ncep.noaa.gov/data/teledoc/telecontents.shtml). The PJ index is identified as the difference in the OLR anomaly between 16°–20°N, 142°–150°E and 32°–38°N, 134°–142°E, based on the definition in Nitta (1987). Basically, the Niño-3 index has quite low degrees of freedom in comparison with $N - 2$ degrees of freedom (where N is the sample size). To assess the significance of the correlations with Niño-3 index, the effective number of degrees of freedom N_e was also computed, which is based on the autocorrelation functions suggested by

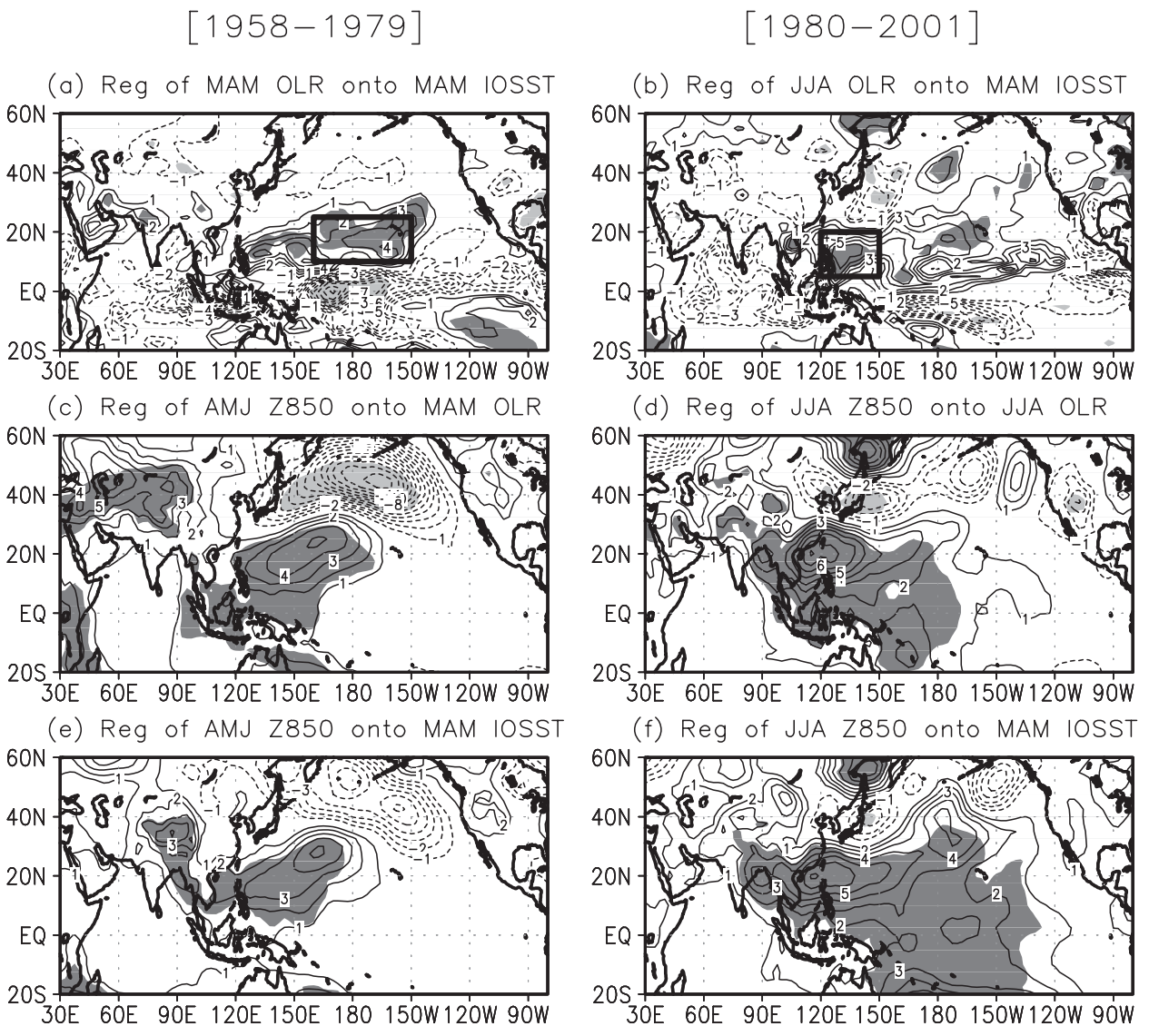

FIG. 8. (a) March–May (MAM) and (b) JJA OLR anomalies regressed against the MAM IOSST anomalies averaged over 20°S–20°N, 50°–100°E during (a) 1958–79 and (b) 1980–2001. (c) April–June (AMJ) and (d) JJA 850-hPa geopotential height anomalies regressed against the (c) MAM and (d) JJA OLR anomalies averaged over the region shown by the black box during (c) 1958–79 and (d) 1980–2001. (e) AMJ and (f) JJA 850-hPa geopotential height anomalies regressed against the MAM IOSST anomalies during (e) 1958–79 and (f) 1980–2001. Shading denotes anomalies significant at the 95% confidence level.

Davis (1976). Overall, the correlation coefficients significant for the N_e (i.e., open circle) are identical to those significant for the $N - 2$ degrees of freedom (i.e., horizontal dashed line), which indicates the significant interdecadal change in the relationship, regardless of the low degrees of freedom. As shown in a previous study (e.g., Horel and Wallace 1981), the WP index is well linked to ENSO, with a peak correlation of ~0.80 (Fig. 9a). Since the late 1970s, however, the correlation between the WP pattern and ENSO has dramatically declined. The weakened link between the WP pattern and ENSO may be due to a stronger Southern Oscillation in the second period. In other words, when the eastern Pacific SST is abnormally warm, the sea level pressure drops in the eastern Pacific and rises in the western Pacific. After the late 1970s, the dominant east–west pressure structure may interrupt the formation of a clear north–south dipole pattern (i.e., WP pattern). Of particular interest is that the relationship between the May–June NPISO activity and WP pattern also dropped off abruptly after the late 1970s. Basically, the temporal correlation coefficient between the early NPISO and the WP pattern during the first and second periods (each containing 22 years) changes from 0.57 in the former period to 0.14 in

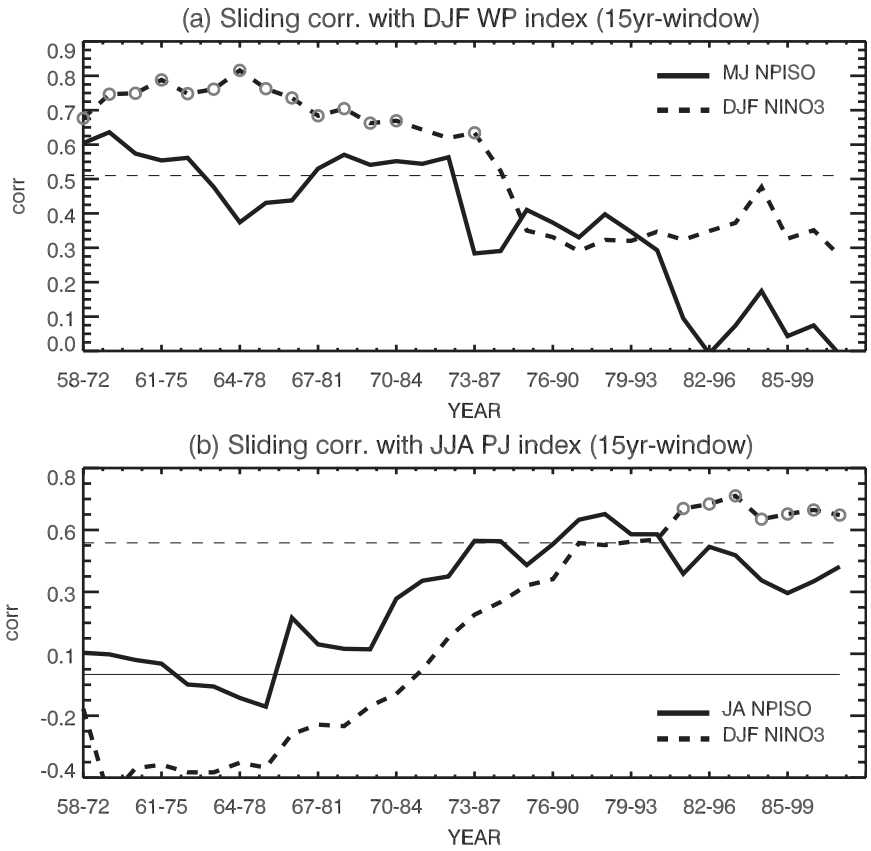

FIG. 9. (a) Sliding correlation between the DJF WP index and the May–June NPISO (solid line) and the DJF Niño-3 index (dashed line) with a 15-yr window. (b) Sliding correlation between the JJA PJ index and the July–August NPISO (solid line) and the DJF Niño-3 index (dashed line) with a 15-yr window. The horizontal dashed line represents values significant at the 95% confidence level for the $N - 2$ degrees of freedom, and the open circle indicates the values significant at the 95% confidence level for the effective number of degrees of freedom.

the latter. This indicates that in the first period, ENSO is closely linked to the WP pattern during winter until spring and then affects the early summer NPISO activity via Rossby wave propagation toward the north. Thus, the ENSO–NPISO relationship may be restricted to only early summer.

While the ENSO–WP link becomes weakened after the late 1970s, the ENSO–PJ relationship becomes strengthened in the second period (Fig. 9b). As the relationship between ENSO and the PJ pattern increases with time, the summer NPISO activity is also significantly correlated to the PJ index with time. The temporal correlation coefficient between the July–August NPISO and the PJ index during the two interdecadal epochs was also changed from −0.04 to 0.57 from the first to the second period. A possible cause for the increasing relationship has been explained by persistent ENSO-induced convection and circulation anomalies over the WNP due to stronger positive feedback between the ocean and atmosphere. The significant change in the summer WNP convection and circulation may considerably contribute to changes in the NPISO–ENSO relationship.

5. Discussion and conclusions

The interdecadal change in the NPISO–ENSO relationship over the EASM system has been explored using ERA-40 OLR data for a period of 44 years (1958–2001). It is well known that the EASM rainfall itself experienced a significant change after the late 1970s (e.g., Hu 1997; Gong and Ho 2002). Unlike the remarked changes in the seasonal mean rainfall and ISV, the interannual variability in the NPISO activity does not show significant interdecadal change. However, the relationship between the NPISO and ENSO has markedly changed since the late 1970s. Although this relationship appears to have changed significantly after the late 1980s (see Fig. 2d), the NPISO–ENSO relationships during both early and late summer had already changed after the late 1970s (not shown). In addition, most of the ENSO-related signals

(e.g., IOSST warming, WNPSH, the suppressed convection over the Philippine Sea) have significantly changed after the late 1970s (e.g., Hu 1997; Gong and Ho 2002; Wu and Wang 2002). Because the interdecadal change in the NPISO–ENSO relationship is considerably attributed to that in the ENSO-related signals, we consider the late 1970s as the change point.

For the years 1958–79, ENSO affected the early summer NPISO. The connection between ENSO and NPISO can be explained by the spring IOSST warming and central North Pacific suppressed convection anomalies. The May–June NPISO activity is consequently related to the ENSO-induced WP pattern in winter until late spring. Note that the WP pattern is clearly linked to the Bonin high, which immediately affects the EASM rainfall as a standing high over the south of Japan (Ha and Lee 2007). During early summer, which is the onset time of the EASM, the significant link between the WP pattern and Bonin high weakened after the late 1970s, which is consistent with the interdecadal change in the NPISO–WP relationship. In addition, Mao et al. (2010) reported that the ISO over East Asia was significantly modulated by intraseasonal variances in the WNPSH, which are closely related to the variation in the Bonin high. The early summer NPISO activity may be connected to the WP pattern in response to the Bonin high. After the late 1970s, however, a strong Southern Oscillation phase tends to interrupt the generation of the WP pattern, which should be investigated in more detail in a future study.

For the years 1980–2001, the boreal summer NPISO activity in July–August was affected by the extreme phase of ENSO of the preceding winter. The relationship during this period is in good agreement with recent studies on the EASM–ENSO relationship (e.g., Chang et al. 2000; Wang et al. 2008), which has become stronger in recent years. This strong EASM–ENSO relationship may have originated from a stronger anomalous Walker–Hadley circulation due to a warmer mean SST. A strong Walker–Hadley circulation has been shown to lead to more persistent ENSO-induced IOSST warming and suppressed convection anomalies over the Philippine Sea. Consequently, ENSO affects the enhanced NPISO activity via the IOSST–WNPSH–NPISO linkage, with the main process being that of the PJ pattern-like teleconnection. In detail, the stationary warm IOSST promotes a stronger chain reaction process such as the IOSST warming–suppressed convection–WNPSH relation. Regarding this mechanism, a controversial question remains: to what degree does the IOSST play a role? In other words, the local cooling over the WNP may be significantly related to the anticyclonic anomalies over the WNP via the air–sea interaction mechanism (e.g., Wang et al. 2000, 2003). To address the question, comprehensive understanding of both observational analyses and numerical experiments will be required in future studies.

After the late 1970s, the WNPSH significantly strengthened with a westward expansion. Along the northern edge of the WNPSH, in the cases of El Niño, the easterly vertical wind shear (i.e., U200–U850) extends north of ~25°N, while in the cases of La Niña westerly vertical wind shear exists in the WNP (i.e., 25°–30°N, 120°–160°E). The westward expansion of the WNPSH is consistent with the vertical shear mechanism (i.e., the vertical shear of zonal flow acts to force the emanation of heating-induced barotropic Rossby waves toward the north) suggested by Wang and Xie (1996). During 1980–2001, the vertical wind shear anomalies and July–August NPISO activity are also negatively correlated, with a peak correlation of approximately −0.6. The marked easterly vertical shear of ~25°N supports the physical mechanism suggested above. However, during 1958–79, the basic state of the vertical wind shear during the active NPISO period only shows a westerly vertical shear north of ~25°N, suggesting that Rossby wave propagation toward the north is somehow suppressed by the basic state of the vertical shear.

Although the OLR data used include some errors in the NPISO activity, these OLR data derived from ERA-40 reproduce a meaningful dynamic relationship between the NPISO and ENSO. This study suggests a seasonal dependence in the NPISO–ENSO relationship and the related interdecadal mechanism change in terms of both WP and PJ patterns. Interestingly, the interdecadal shift from early to late summer in the NPISO–ENSO relationship is reasonably consistent with a temporal shift of peak rainfall in the EASM (e.g., Gong and Ho 2002; Ha et al. 2005). The link between the change in the seasonal mean rainfall and the NPISO activity as well as the NPISO–ENSO relationships should be investigated in more detail in future studies; furthermore, the detailed dynamical process will be also examined using general circulation models.

Acknowledgments. This work was supported by the Ministry of the Environment as ''The Eco-technopia 21 project'' and by a Korea Research Foundation Grant funded by the South Korean Government (MOEHRD) (KRF-2007-313-C00783), as well as by the second stage of the Brain Korea 21 Project in 2009.

REFERENCES

Chang, C.-P., Y. Zhang, and T. Li, 2000: Interannual and interdecadal variations of the East Asian summer monsoon and tropical Pacific SSTs. Part I: Roles of the subtropical ridge. *J. Climate,* **13,** 4310–4325.

Davis, R. E., 1976: Predictability of sea surface temperature and sea level pressure anomalies over the North Atlantic. *J. Phys. Oceanogr.,* **6,** 249–266.

Ding, R., K.-J. Ha, and J. Li, 2010: Interdecadal shift in the relationship between the East Asian summer monsoon and the tropical Indian Ocean. *Climate Dyn.,* **34,** 1059–1071.

Gong, D.-Y., and C.-H. Ho, 2002: Shift in the summer rainfall over the Yangtze River valley in the late 1970s. *Geophys. Res. Lett.,* **29,** 1436, doi:10.1029/2001GL014523.

Goswami, B. N., and R. S. A. Mohan, 2001: Intraseasonal oscillations and interannual variability of the Indian summer monsoon. *J. Climate,* **14,** 1180–1198.

Ha, K.-J., and E. Ha, 2006: Climatic change and interannual fluctuation in the long-term record of monthly precipitation for Seoul. *Int. J. Climatol.,* **26,** 607–618.

——, and S.-S. Lee, 2007: On the interannual variability of the Bonin high associated with the East Asian summer monsoon rain. *Climate Dyn.,* **28,** 67–83.

——, S.-K. Park, and K.-Y. Kim, 2005: On interannual characteristics of Climate Prediction Center merged analysis precipitation over the Korean peninsula during the summer monsoon season. *Int. J. Climatol.,* **25,** 99–116.

Hendon, H. H., C. Zhang, and J. D. Glick, 1999: Interannual variation of the Madden–Julian oscillation during austral summer. *J. Climate,* **12,** 2538–2550.

Horel, J. D., and J. M. Wallace, 1981: Planetary-scale atmospheric phenomena associated with the Southern Oscillation. *Mon. Wea. Rev.,* **109,** 813–829.

Hsu, H.-H., and C.-H. Weng, 2001: Northwestward propagation of the intraseasonal oscillation in the western North Pacific during the boreal summer: Structure and mechanism. *J. Climate,* **14,** 3834–3850.

Hu, Z.-Z., 1997: Interdecadal variability of summer climate over East Asia and its association with 500-hPa height and global sea surface temperature. *J. Geophys. Res.,* **102** (D16), 19 403–19 412.

Jiang, X., T. Li, and B. Wang, 2004: Structures and mechanisms of the northward propagating boreal summer intraseasonal oscillation. *J. Climate,* **17,** 1022–1039.

Kalnay, E., and Coauthors, 1996: The NCEP/NCAR 40-Year Reanalysis Project. *Bull. Amer. Meteor. Soc.,* **77,** 437–471.

Kang, I.-S., C.-H. Ho, Y.-K. Lim, and K.-M. Lau, 1999: Principal mode of climatological seasonal and intraseasonal variations of the Asian summer monsoon. *Mon. Wea. Rev.,* **127,** 322–340.

Kawamura, R., T. Murakami, and B. Wang, 1996: Tropical and midlatitude 45-day perturbations over the western Pacific during the northern summer. *J. Meteor. Soc. Japan,* **74,** 867–890.

Kemball-Cook, S., and B. Wang, 2001: Equatorial waves and air–sea interaction in the boreal summer intraseasonal oscillation. *J. Climate,* **14,** 2923–2942.

Kim, H.-M., I.-S. Kang, B. Wang, and J.-Y. Lee, 2008: Interannual variations of the boreal summer intraseasonal variability predicted by ten atmosphere–ocean coupled models. *Climate Dyn.,* **30,** 485–496.

Klein, S. A., B. J. Soden, and N.-C. Lau, 1999: Remote sea surface temperature variations during ENSO: Evidence for a tropical atmospheric bridge. *J. Climate,* **12,** 917–932.

Lau, K.-M., and P. H. Chan, 1986: Aspects of the 40–50-day oscillation during the northern summer as inferred from outgoing longwave radiation. *Mon. Wea. Rev.,* **114,** 1354–1367.

——, G. J. Yang, and S. H. Shen, 1988: Seasonal and intraseasonal climatology of summer monsoon rainfall over East Asia. *Mon. Wea. Rev.,* **116,** 18–37.

Li, Y., R. Lu, and B. Dong, 2007: The ENSO–Asian monsoon interaction in a coupled ocean–atmosphere GCM. *J. Climate,* **20,** 5164–5177.

Mao, J., Z. Sun, and G. Wu, 2010: 20–50-day oscillation of summer Yangtze rainfall in response to intraseasonal variations in the subtropical high over the western North Pacific and South China Sea. *Climate Dyn.,* **34,** 747–761, doi:10.1007/s00382-009-0628-2.

Nitta, T., 1987: Convective activities in the tropical western Pacific and their impact on the Northern Hemisphere summer circulation. *J. Meteor. Soc. Japan,* **65,** 373–390.

North, G. R., T. L. Bell, F. J. Moeng, and R. F. Cahalan, 1982: Sampling errors in the estimation of empirical orthogonal functions. *Mon. Wea. Rev.,* **110,** 699–706.

Quan, X.-W., H. F. Diaz, and C.-B. Fu, 2003: Interdecadal change in the Asia–Africa summer monsoon and its associated changes in global atmospheric circulation. *Global Planet. Change,* **37,** 171–188.

Rayner, N. A., D. E. Parker, E. B. Horton, C. K. Folland, L. V. Alexander, D. P. Rowell, E. C. Kent, and A. Kaplan, 2003: Global analyses of sea surface temperature, sea ice, and night marine air temperature since the late nineteenth century. *J. Geophys. Res.,* **108,** 4407, doi:10.1029/2002JD002670.

Seo, K.-H., J.-K. E. Schemm, W. Wang, and A. Kumar, 2007: The boreal summer intraseasonal oscillation simulated in the NCEP Climate Forecast System: The effect of sea surface temperature. *Mon. Wea. Rev.,* **135,** 1807–1827.

——, W. Wang, J. Gottschalck, Q. Zhang, J.-K. E. Schemm, W. R. Higgins, and A. Kumar, 2009: Evaluation of MJO forecast skill from several statistical and dynamical forecast models. *J. Climate,* **22,** 2372–2388.

Slingo, J. M., D. P. Rowell, K. R. Sperber, and F. Nortley, 1999: On the predictability of the interannual behaviour of the Madden–Julian Oscillation and its relationship with El Niño. *Quart. J. Roy. Meteor. Soc.,* **125,** 583–609.

Teng, H., and B. Wang, 2003: Interannual variations of the boreal summer intraseasonal oscillation in the Asian–Pacific region. *J. Climate,* **16,** 3572–3584.

Terao, T., and T. Kubota, 2005: East–west SST contrast over the tropical oceans and the post El Niño western North Pacific summer monsoon. *Geophys. Res. Lett.,* **32,** L15706, doi:10.1029/2005GL023010.

Trenberth, K. E., and J. W. Hurrell, 1994: Decadal atmosphere–ocean variations in the Pacific. *Climate Dyn.,* **9,** 303–319.

Uppala, S. M., and Coauthors, 2005: The ERA-40 Re-Analysis. *Quart. J. Roy. Meteor. Soc.,* **131,** 2961–3012.

Wallace, J. M., and D. S. Gutzler, 1981: Teleconnections in the geopotential height field during the Northern Hemisphere winter. *Mon. Wea. Rev.,* **109,** 784–812.

Wang, B., 1995: Interdecadal changes in El Niño onset in the last four decades. *J. Climate,* **8,** 267–285.

——, and X. Xie, 1996: Low-frequency equatorial waves in vertically sheared zonal flow. Part I: Stable waves. *J. Atmos. Sci.,* **53,** 449–467.

——, and ——, 1997: A model for the boreal summer intraseasonal oscillation. *J. Atmos. Sci.,* **54,** 72–86.

——, R. Wu, and X. Fu, 2000: Pacific–East Asian teleconnection: How does ENSO affect East Asian climate? *J. Climate,* **13,** 1517–1536.

——, ——, and T. Li, 2003: Atmosphere–warm ocean interaction and its impacts on Asian–Australian monsoon variation. *J. Climate,* **16,** 1195–1211.

——, J.-G. Jhun, and B.-K. Moon, 2007: Variability and singularity of Seoul, South Korea, rainy season (1778–2004). *J. Climate,* **20,** 2572–2580.

——, J. Yang, and T. Zhou, 2008: Interdecadal changes in the major modes of Asian–Australian monsoon variability: Strengthening relationship with ENSO since the late 1970s. *J. Climate,* **21,** 1771–1789.

Watanabe, M., and F.-F. Jin, 2002: Role of Indian Ocean warming in the development of Philippine Sea anticyclone during ENSO. *Geophys. Res. Lett.,* **29,** 1478, doi:10.1029/2001GL014318.

Webster, P. J., 1983: Mechanisms of monsoon low-frequency variability: Surface hydrological effects. *J. Atmos. Sci.,* **40,** 2110–2124.

Wu, R., and B. Wang, 2002: A contrast of the East Asian summer monsoon–ENSO relationship between 1962–77 and 1978–93. *J. Climate,* **15,** 3266–3279.

Xie, S.-P., K. Hu, J. Hafner, H. Tokinaga, Y. Du, G. Huang, and T. Sampe, 2009: Indian Ocean capacitor effect on Indo–western Pacific climate during the summer following El Niño. *J. Climate,* **22,** 730–747.

Yun, K.-S., K.-H. Seo, and K.-J. Ha, 2008: Relationship between ENSO and northward propagating intraseasonal oscillation in the East Asian summer monsoon system. *J. Geophys. Res.,* **113,** D14120, doi:10.1029/2008JD009901.

——, B. Ren, K.-J. Ha, J. C. L. Chan, and J.-G. Jhun, 2009: The 30–60-day oscillation in the East Asian summer monsoon and its time-dependent association with the ENSO. *Tellus,* **61A,** 565–578.

Zhang, Y., J. M. Wallace, and D. S. Battisti, 1997: ENSO-like interdecadal variability: 1900–93. *J. Climate,* **10,** 1004–1020.

Zveryaev, I. I., 2002: Interdecadal changes in the zonal wind and the intensity of intraseasonal oscillations during boreal summer Asian monsoon. *Tellus,* **54A,** 288–298.